Applied Catalysis B: Environmental 249 (2019) 211–217

Contents lists available at ScienceDirect

Applied Catalysis B: Environmental

journal homepage: www.elsevier.com/locate/apcatb

Performance and kinetic modelling of photolytic and photocatalytic ozonation for enhanced micropollutants removal in municipal wastewaters

Danilo Bertagna Silva, Alberto Cruz-Alcalde, Carmen Sans, Jaime Giménez*, Santiago Esplugas

Department of Chemical Engineering and Analytical Chemistry, Faculty of Chemistry, Universitat de Barcelona, C/Martí i Franqués 1, 08028 Barcelona, Spain

ARTICLE INFO

Keywords:
Wastewater ozonation
UV light
Photocatalysis
Advanced oxidation processes
Recalcitrant micropollutants

ABSTRACT

In this work, the performances of ozonation, photolytic ozonation (UV-C/O_3), and photocatalytic ozonation (UV-A/TiO_2/O_3) in degrading ozone recalcitrant micropollutants in four different real domestic wastewaters were evaluated in semi-continuous operation, together with the influence of water matrices in the ozone mass transfer and pollutant degradation rates. The ˙OH exposure per consumed ozone ratio, defined as $R_{OH,O3}$, was applied for single ozonation and modified for light-assisted ozonation processes to evaluate and compare the contribution of radical pathway on micropollutants abatement for the different wastewaters studied. $R_{OH,O3}$ plots presented good fitting ($R^2 > 0.95$) in two stages, corresponding to different ozone mass transfer regimes, for all cases. Light-assisted ozonation attained higher pollutant degradation for all water matrices compared to single ozonation, although the performance of UV-assisted processes was more sensitive to matrix factors like composition and turbidity. Moreover, the improvement brought by both light-based processes on R_{OHO3} values mainly took place during the second stage. Thus, photocatalytic ozonation reached R_{OHO3} values higher than double for all wastewaters, compared with single ozonation (between 105% and 127% increase). These values represent a saving of almost half of the overall ozone needs (42%) for the same ozone recalcitrant micropollutant depletion, although it would require the adoption of higher ozone doses than the currently employed for ozonation in wastewater treatment plants.

1. Introduction

The ever-growing development, production and consumption of new chemical substances have raised the need of developing new technologies for wastewater treatment because many of these substances show a bio-accumulative and non-biodegradable character, persisting in the environment [1]. These substances are commonly called micropollutants (MP) because their presence on water bodies and wastewater treatment plants (WWTP) effluents ranges from nano ($ng\,L^{-1}$) to micro ($\mu g\,L^{-1}$) scale [2,3]. Their presence in the aquatic environment is associated to a variety of negative effects, including short and long-term toxicity, endocrine disruption and antibiotic resistance in microorganisms [4,5].

The high oxidation potential of ozone (O_3) makes it an effective tool for wastewater treatment, with demonstrated performance by many studies from laboratory to full scale [6–8]. The quick decomposition of ozone leaves no traces of its presence in water, unlike chlorine. However, ozone is a selective oxidant. Second-order rate constants for ozone vary several orders of magnitude, between $< 0.1\,M\,s^{-1}$ and $7 \times 10^9\,M\,s^{-1}$ [9]. Due to its high production costs, ozone doses typically employed are relatively low: TOD/DOC (transferred ozone dose/dissolved organic carbon) ratios range between 0.5 and 1.5 [10].

The stress caused by global water scarcity has been increasing demands of wastewater reuse for direct human consumption [11]. Therefore, higher purity standards have to be attained to eliminate all pollutants and allow a safe use of water. Higher O_3 doses can be a way of reaching this goal, because the natural decomposition of ozone generates hydroxyl radicals (˙OH) in non-acidic pHs (Eqs. (1) and (2)). These radicals have a higher oxidation potential than ozone and they are non-selective oxidants, being able to oxidize many molecules that ozone cannot. Therefore, this is an interesting option for the abatement of recalcitrant micropollutants and attain a high level of water purity [12].

$$O_3 + OH^- \rightarrow HO_2^- + O_2 \quad (1)$$

$$O_3 + HO_2^- \rightarrow OH\cdot + O_2^{\cdot -} + O_2 \quad (2)$$

Degradation of a micropollutant during ozonation can be described by Eq. (3), accounting for the sum of molecular ozone and hydroxyl radicals contribution [13]. There is a considerable number of data on

* Corresponding author.
E-mail address: j.gimenez@ub.edu (J. Giménez).

https://doi.org/10.1016/j.apcatb.2019.02.072
Received 28 September 2018; Received in revised form 21 February 2019; Accepted 26 February 2019
Available online 27 February 2019
0926-3373/ © 2019 Elsevier B.V. All rights reserved.

kinetic constants of pollutants reactions with molecular ozone and the hydroxyl radical [14,15], being those for hydroxyl radical in the range of 10^9–10^{10} M s^{-1} for most of micropollutants.

$$-\ln\left(\frac{[MP]}{[MP]_0}\right) = k_{MP,O_3}\int [O_3]\,dt + k_{MP,OH\cdot}\int [OH\cdot]\,dt \quad (3)$$

Ultra-violet light is commonly adopted on wastewater treatment plants for disinfection [16]. Many pollutants and cell membranes of microorganisms undergo photolysis. Their degradation rates vary with light intensity and wavelength, matrix composition and geometry of the reactor [17].

Ozone absorbs light at UV-C range, presenting a peak value at wavelength of 254 nm [12]. Eqs. (4)–(6) show the formation of hydroxyl radicals under these circumstances [18], creating a highly oxidative medium in a process called photolytic ozonation.

$$O_3 + H_2O \xrightarrow{h\nu} O_2 + H_2O_2 \quad (4)$$

$$H_2O_2 \xrightarrow{h\nu} 2OH\cdot \quad (5)$$

$$2O_3 + H_2O_2 \rightarrow 2OH\cdot + 3O_2 \quad (6)$$

Besides contributing on radical formation, when UV light is included in the system, a first-order degradation rate photolysis of a target micropollutant should be accounted on the equation describing its abatement [18] (Eq. (7)).

$$-\ln\left(\frac{[MP]}{[MP]_0}\right) = k_{MP,O_3}\int [O_3]dt + k_{MP,OH\cdot}\int [OH\cdot]dt + k_{MP,UV}\int dt \quad (7)$$

The high photocatalytic activity of TiO_2 and some of its properties (economical, non-toxic, insoluble and stable in water [19]) make it a substance of great interest for wastewater treatment and recalcitrant pollutants abatement. With a band gap between 3.0 and 3.2 eV (UV-A, near visible), electrons on its valence band (e_{vb}^-) can be promoted to conduction band (e_{cb}^-), generating a reactive electron-hole pair when irradiated by UV light [20]. This pair can go back to its original place or engage in oxidation reactions with the surrounding medium. In wastewater matrices, this can generate hydroxyl radicals and contribute to micropollutants abatement [21,22].

Ozonation and photocatalysis can be combined to attain a higher degree of pollutant degradation in a process called photocatalytic ozonation. Ozone reacts with the conductive-band electron, thus preventing its return to the valence band, and forms ozonide radicals (O_3^-), an initial step towards the formation of more hydroxyl radicals in this system, shown by Eqs. (8) and (9) [23–25]. The degradation efficiency of photocatalytic ozonation has been demonstrated in many lab-scale studies [26–30], but few of them have been performed on real wastewaters [31,32].

$$O_3 + e^- \rightarrow O_3^-\cdot \quad (8)$$

$$O_3^-\cdot + H_2O \rightarrow O_2 + OH^- + OH\cdot \quad (9)$$

The control of micropollutants removal and the optimization of the required ozone dose during the process are still unaccomplished challenges. One of the most common difficulties is the impossibility of directly measuring the hydroxyl radical concentration, due to its nearly instantaneous reaction rates [33,34]. Attempts to work around this problem were made by the development of the recent R_{OHO3} concept, which is a valuable step towards the prediction of pollutant abatement in ozonation processes [35]. The R_{OHO3} concept is defined as the hydroxyl radical exposure per transferred ozone dosage (Eq. (10)).

$$R_{OHO_3=}\frac{\int [OH\cdot]dt}{TOD_t} \quad (10)$$

The ·OH exposure can be obtained through the monitoring of a probe compound with $k_{MP,O3} < 10\ M^{-1}\ s^{-1}$ [37]. For those ozone-resistant substances, substituting Eq. (10) on Eq. (7) results in Eq. (11), that can be used to predict pollutant degradation [36]:

$$-\ln\left(\frac{[MP]_t}{[MP]_0}\right) = k_{MP,OH\cdot}{*}R_{OH,O_3}{*}TOD_t \quad (11)$$

The goals of this study were: 1) to compare the performance of single, photolytic and photocatalytic removal of ozone-resistant micropollutants in real municipal wastewaters coming from different sources and processes, thus having very different compositions; 2) to adapt and check the utility of the R_{OHO3} concept in the modelling of these ozone-based processes; 3) to evaluate the influence of light and catalyst on the ozonation of different real domestic wastewaters trough the R_{OHO3} parameter.

2. Materials and methods

2.1. Chemical and reagents

Acetamiprid (ACMP) and atrazine (ATZ) analytical standards were acquired from Sigma-Aldrich (Germany). Ultrapure water was produced in site by a filtration system (Millipore, USA). Pure oxygen (≥ 99.99%) was supplied by Abelló Linde (Spain). Titanium Dioxide P-25 was supplied by Evonik (primary particle size of 21 nm).

2.2. Wastewater characterization

Four wastewater effluents were employed in this work from two different WWTPs in Gavà and El Prat (Barcelona, Spain). Two of them came from Gavà station (MBR – outlet of a membrane bioreactor, MBBR – outlet of a moving bed biofilm reactor) and the other two came from El Prat station (CAS – conventional activated sludge, CAS-DN - conventional activated sludge with denitrification). Their main quality parameters are gathered in Table 1. (TOC: total organic carbon; COD: chemical oxygen demand; UV_{254}: specific absorbance at 254 nm) All the effluent samples were filtered with conventional filter paper, to remove coarse particles, and stored at 4 °C prior to use.

2.3. Single and light assisted ozonation experiments

Ozone was produced from pure oxygen by a 301.19 lab ozonizer (Sander, Germany). The ozonation of wastewaters was performed in a 1.5 L jacketed reactor covered with aluminum foil, to avoid radiation losses, and operated in semi-continuous mode. Ozone was injected at the bottom of the reactor by a porous diffuser. A magnetic stirrer ensured the good contact between liquid and gas phases and a homogeneous liquid phase. Experiments were performed at 22 ± 2 °C. The gas flow rate was maintained at 0.3 L min^{-1} and the inlet concentration

Table 1
Effluent characterization.

Wastewater ID	pH	Turbidity [NTU]	TOC [mg C L^{-1}]	COD [mg O_2 L^{-1}]	UV_{254} [m^{-1}]	DOC [mg C L^{-1}]	Alkalinity [mg $CaCO_3$ L^{-1}]
MBR	7.7	0.5	13.6	14.9	17.4	13.3	208
CAS-DN	7.5	2.6	13.2	27.3	24.6	13.4	275
CAS	8.0	20.1	37.8	70.5	48.9	18.7	449
MBBR	7.8	18.5	51.1	71.3	50.3	21.7	469

of ozone at 10 mg L^{-1} (values at STP conditions). Gas-phase ozone concentrations were continuously monitored by two BMT 964 ozone analyzers (BMT Messtechnik, Germany) placed on the reactor inlet and outlet. The ozone concentration in the liquid phase was measured by a Q45H/64 dissolved O_3 probe (Analytical Technology, USA), which was connected to a liquid recirculation stream. For experiments with TiO_2, the dissolved ozone was not measured to preserve the equipment's probe membranes from small solid particles.

A detailed scheme of the ozonation setup is shown elsewhere [36].

For experiments assisted by UV radiation, two different reactor configurations were employed. In experiments with UV-C radiation, a single lamp (4 W, 254 nm, Phillips) with a photon fluence rate of 1.01 mW cm^{-2} (obtained by atrazine's actinometry [37]) was used. For experiments with UV-A light, three black light bulb (BLB) lamps (Philips TL 8 W-08 FAM) of 8 W each with a wavelength range 350–400 nm (maximum at 365 nm) and a fluence rate of 5.47 mW cm^{-2} were used instead. In both cases, the lamps – protected by means of quartz sleeves – were immersed and placed at the center of the reaction vessel. Prior to start experiments, they were turned on for 20 min to attain a constant photon flow.

For experiments using titanium dioxide, its addition to the reaction medium was made at the concentration of 0.1 g L^{-1}. A magnetic stirrer homogenized the system for 20 min prior to the beginning of treatment.

The transferred ozone dose (TOD), which represents the accumulated amount of ozone that is transferred to reactor per unit of volume during a given time, was determined as explained in Supplementary information (Text S1) [38].

All experiments ran for one hour. ACMP was used as ˙OH probe compound, since it is an O_3-resistant micropollutant ($k_{ACMP,O3} = 0.25\ M^{-1}\ s^{-1}$ and $k_{ACMP,\cdot OH} = 2.1{\cdot}10^{9}\ M^{-1}\ s^{-1}$) [39]. The spiked concentration of ACMP in all effluents was 100 µg L^{-1}. Samples were withdrawn at known time intervals and kept at room conditions until complete consumption of dissolved ozone was achieved.

On each sample, the residual concentration of ACMP was measured by HPLC-UV [39]. Prior to the analysis, samples were filtered using 0.45 µm PVDF syringe filters.

All different ozonation processes and the corresponding blank experiments were also performed on Milli-Q water buffered with a pH 7 phosphate solution (1 M). The results can be found on the Supplementary information, Figs. S1 and S2.

3. Results and discussion

3.1. Ozone mass transfer and ozone demand

Ozone mass balance and demand could be assessed through continuously monitoring inlet and outlet (gas phase) ozone concentrations, as well as dissolved (liquid phase) ozone (Figs. S3–S7). Clearly, two kinetic regimes could be discerned: initially, ozone mass transfer was very fast, attaining a η_{tr} value (slope of transferred versus applied ozone doses plot) above 0.8 for all matrices and processes (see Table 2 and Fig. S8 on the SI). During the first stage, all wastewaters contained substances that are highly reactive with ozone, consuming it faster. In the second stage, encompassing the last 30 min of experiment, the transfer yield decreased because it got controlled by moderate or slow ozone rate reactions [12] and it was possible to discern the influence of different matrices: wastewaters with a higher organic and inorganic carbon content (CAS and MBBR) had higher ozone transfer yields.

When UV-C light was turned on, the η_{tr} value increased for all wastewaters in the second stage. UV-C light accelerates ozone depletion (Eq. (4)) leading to less ozone leaving the system, thus optimizing the transfer yield for all cases. Ozone transfer yield increase was higher for less turbid matrices, Milli-Q, MBR and CAS-DN, due to the better UV-C radiation transmission on these media.

When UV-A was added to TiO_2 experiments, ozone mass transfer of the Milli-Q, MBR and CAS-DN matrices improved considerably. Less turbidity and lower organic matter content (see Table 1) allowed more photon absorption by TiO_2, leading to a higher e^-_{cb} production. Eq. (8) shows how this may lead to additional ozone consumption in the system.

Table 2
O_3 mass transfer, IOD and k_d for all studied waters. All $R^2 > 0.99$.

Process	MATRIX ID	η_{tr} [trans. O_3/app. O_3]		IOD [mgO_3 L^{-1}]	k_d [min^{-1}]
		Stage 1	Stage 2		
Ozonation	Milli-Q	0.86	0.14	4	0.10
UV-C/O_3		0.90	0.40	–	–
TiO_2/O_3		0.89	0.04		
TiO_2/UV-A/O_3		0.87	0.40		
Ozonation	MBR	0.82	0.17	12	0.14
UV-C/O_3		0.82	0.37	–	–
TiO_2/O_3		0.87	0.14		
TiO_2/UV-A/O_3		0.83	0.35		
Ozonation	CAS-DN	0.88	0.17	15	0.05
UV-C/O_3		0.91	0.41	–	–
TiO_2/O_3		0.82	0.20		
TiO_2/UV-A/O_3		0.80	0.29		
Ozonation	CAS	0.85	0.30	18	0.29
UV-C/O_3		0.89	0.44	–	–
TiO_2/O_3		0.88	0.27		
TiO_2/UV-A/O_3		0.83	0.30		
Ozonation	MBBR	0.88	0.31	25	0.54
UV-C/O_3		0.94	0.37	–	–
TiO_2/O_3		0.95	0.27		
TiO_2/UV-A/O_3		0.85	0.28		

Table 2 also includes the instantaneous ozone demand (IOD) and the pseudo-first order decay rate of ozone (k_d) values obtained for ozonation (for definition and calculation methods see Text S1). Values for photolytic ozonation were not obtained because no ozone was detected in the liquid phase during those experiments due to the efficient ozone decomposition under those integrated systems. IOD describes the ozone demand when it is instantaneously consumed by the wastewater, and consequently represents the dose of ozone at the point of the transition between primary (fast) and secondary (slow) ozonation stages [38]. As it is expected, more polluted matrices had higher IODs. For real wastewaters, an IOD/DOC ratio of approximately 1.0 ± 0.1 was obtained for all wastewaters tested. Milli-Q water presented two phases and IOD value of 4 mg/L due to the ACMP addition.

k_d values were higher for more polluted water, but since the TOC value of MBR and CAS-DN are similar, the latter had a slower O_3 decomposition due to its higher alkalinity content [40].

3.2. Degradation of a model O3-resistant compound: ACMP

First of all, control tests for UV-A and UV-C photolysis and UV-A/TiO_2 photocatalysis were performed to verify their contribution on photocatalytic ozonation. ACMP did not show any degradation due to UV-A photolysis, and UV-A/TiO_2 photocatalysis presented little degradation for the MBR effluent sample (less than 6%) and no degradation for all the other wastewaters (Fig. S9 of the Supplementary information). ACMP degradation by UV-C radiation ranked from 45% for MBBR up to 60% for MBR, increasing with the decrease of organic matter content and turbidity of wastewater (Fig. S10).

Fig. 1 shows degradation of ACMP for single, photolytic (UV-C), photocatalytic (UV-A/TiO_2) and catalytic (TiO_2) ozonation in all matrices tested, at different TOD/DOC ratios. Fig. S11 shows the same degradation per reaction time (60 min).

TiO_2/O_3 did not bring any clear improvement with respect to single ozonation. However, photo-assisted processes significantly improved the abatement of ACMP, demonstrating the enhanced ˙OH production. Photolytic ozonation showed final ACMP degradations above 90% for all matrices. Photocatalytic ozonation was the most matrix-influenced

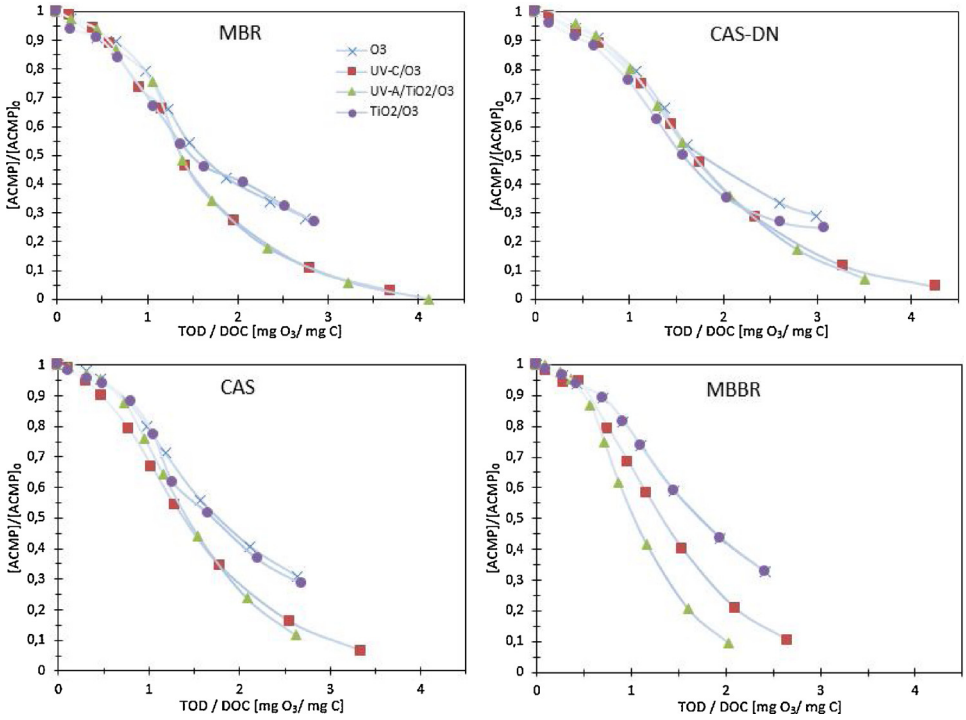

Fig. 1. ACMP degradation per TOD/DOC_0 ratio for all studied wastewaters. Gas flow rate = 0.3 L min^{-1}; Inlet (g) ozone concentration = 10 mg O_3 L^{-1}; $T_{reaction}$ = 20 ± 2 °C; T_{in} (gas) = 22 ± 2 °C; P_{in} (gas) = 25 ± 2 mbar.

process: MBR matrix reached 100% of ACMP final degradation – being the highest of all the experiments – but this value dropped on each of the other matrices: final degradation in CAS-DN was 93% and in CAS and MBBR, 89%. As more organic matter adsorbed on the catalyst surface hinders its photo-activity, photocatalytic ozonation efficiency decreases. Moreover, turbid matrices also hinder photo-activity, as well as the presence of dissolved UV-absorbent organic species, thus decreasing the amount of photons reaching the catalyst surface.

On Fig. 1 it is possible to see that the two light-based ozonation processes started to improve its effectiveness compared with single ozonation or TiO_2/O_3 at different TOD/COD values. The cleaner matrices MBR and CAS-DN required a TOD/DOC ratio of about 1.5, much higher than currently employed ratios for these types of waters (from 0.5 up to 1). This can be related to the two-stage character of the process: initially, reactivity between O_3 and matrix compounds is very high, hindering radical production with or without light. During second stage, quick O_3 reactions are less prominent and radical formation paths are favored. Moreover, a decrease in turbidity during ozonation would have allowed more photons to reach O_3 or TiO_2 molecules, promoting the radical pathway as well. This means that, in order to improve ozone-resistant micropollutants removal by light assisted processes, the employed ozone doses should also increase. In return, the ozone doses required to reach satisfactory degradation levels of recalcitrant micropollutants will be reduced due to the increase of ˙OH-exposure provided by light assisted processes compared to single ozonation. In the case of ACMP, for 65% of initial concentration removal, the needed TOD/DOC ratio decreased from 2.3 to 1.7 for MBR and from 2.4 to 2.0 for CAS-DN, and consequently the corresponding ozone dose demand for both light assisted processes would be lower (27% and 17%, respectively).

The addition of UV-C light and UV-A/TiO_2 in the more polluted waters CAS and MBBR clearly improved the overall AMCP degradation efficiency from lower TOD/DOC ratios of 1.2 and 0.6, respectively. That is, improvement of ˙OH-exposure provided by light assisted processes were assessed at TOD/COD ratios closer to currently employed ones. Still, due to high organic content and alkalinity of these types of wastewaters, the TOD/DOC needed for recalcitrant micropollutants abatement and consequently the required ozone doses would be much higher. Thus, in the case of 65% removal achievement of initial ACMP concentration, the TOD/COD ratio decreased from 2.2 in single ozonation to 1.7 for light assisted processes in CAS effluent, while for MBBR wastewater, this ratio dropped from 2.4 down to 1.7 for photolysis and to 1.3 for photocatalytic ozonation. The latter represents a saving of almost half of the overall ozone needs (42%) for the same micropollutant degree of depletion.

3.3. R_{OHO3} determination

In this work, the recalcitrant pesticide acetamiprid was used as model compound for R_{OHO3} estimation during wastewater ozonation. UV-C photolysis blank tests were carried out for all wastewaters to quantify their contribution on ACMP degradation during photolytic ozonation (Eq. (7)). The first-order degradation rate $k_{MP,UV}$ obtained for each matrix was used to deduct the amount of hydroxyl radical exposure at each reaction time t, according to Eq. (12). During ozonation the matrices undergo several changes, and it can be a source of error on degradation rate determination [12]. Being so, it is not possible to determine separately how much of acetamiprid degradation is due to direct photolysis and how much to the oxidation by the hydroxyl radical. Thus, factors affecting photolysis were considered constant for all experiments and included in the $k_{MP,UV}$ value.

$$\int [OH\cdot]dt = \frac{\ln\left(\frac{[MP]_t}{[MP]_0}\right) + k_{MP,UV}{}^{*}t}{-k_{MP,OH\cdot}} \quad (12)$$

Data of ˙OH exposure per consumed ozone dose fitted to linear model according to Eq. (10) ($R^2 > 0.95$), obtaining R_{OHO3} values for all water matrices. These are shown on Table 3, and their plots are given on Fig. 2.

Two different ozonation regimes – stage 1 (S1) and stage 2 (S2) – were observed for all tests, corresponding to the two ozone transfer rates previously observed, and two R_{OHO3} values were fitted for each stage. Stage 2 values were higher than stage 1 for all cases. In stage 2, the slower molecular ozone consumption by the matrix allows more

Table 3
R_{OHO3} values for plots on Fig. 2 and TOD to 65% of ACMP degradation. All $R^2 > 0.95$.

Process	Wastewater ID	R_{OHO3} [10^7 s^{-1}]		TOD $_{ACMP\ 65\%}$ [mg O_3 L^{-1}]
		S1	S2	
Ozonation	MBR	3.9	8.9	30
UV-C/O_3		1.6	16.0	22
TiO_2/O_3		4.1	9.0	31
UV-A/TiO_2/O_3		5.1	19.7	22
Ozonation	CAS-DN	2.5	8.5	34
UV-C/O_3		1.6	12.8	28
TiO_2/O_3		3.4	9.1	29
UV-A/TIO_2/O_3		4.5	17.4	28
Ozonation	CAS	2.4	7.0	45
UV-C/O_3		1.7	9.6	33
TiO_2/O_3		1.5	7.2	43
UV-A/TiO_2/O_3		1.4	14.3	33
Ozonation	MBBR	1.7	6.5	50
UV-C/O_3		1.2	9.3	35
TiO_2/O_3		0.8	7.2	53
UV-A/TiO_2/O_3		1.8	14.8	29

radical formation per transferred ozone by the different mechanism involved in the processes, increasing the R_{OHO3}, as previously discussed.

By comparing R_{OHO3} it was possible to verify the matrix influence on radical production: waters with higher alkalinity and organic carbon content had smaller R_{OHO3} values because many organic substances, bicarbonates and carbonates ions are well known radical scavengers [41,42].

Comparing the R_{OHO3} values obtained for single and photolytic ozonation, the latter presented smaller values for stage 1 for all matrices. This can be explained by the hypothesis of a too low concentration of the peroxide generated intermediate. On stage 1 only a small amount of ozone is available for photolysis due to its quick reactivity with the medium, generating a small amount of peroxide (Eq. (4)). While ozone has a high absorptivity at 254 nm in both liquid (3300 M^{-1} cm^{-1}) and gas (2950 M^{-1} cm^{-1}) phases [12], peroxide absorbs at a much lower rate (19 M^{-1} cm^{-1}) [43]. The efficiency of its photolysis (Eq. (5) the final step for radical generation) has been reported to be considerably impaired by the presence of pollutants found on wastewaters, especially for small peroxide concentrations [43,44]. The consequence is that, for stage 1, ozone is being photolyzed (more ozone is being transferred) but less hydroxyl radicals are being formed. Photolysis of ozone reduces the O_3 available for reactions of Eqs. (1) and (2), thus decreasing the hydroxyl radical production and the R_{OHO3} value in comparison to single ozonation. In addition, there is possibly an overestimation of the initial rate of ACMP degradation via direct photolysis, resulting in an underestimation of the total hydroxyl radical exposure value (Eq. (12)). The degradation rate of ACMP was obtained for each matrix in a blank experiment without ozone flow, using only UV light. Since ozone strongly absorbs UV at the 254 nm wavelength

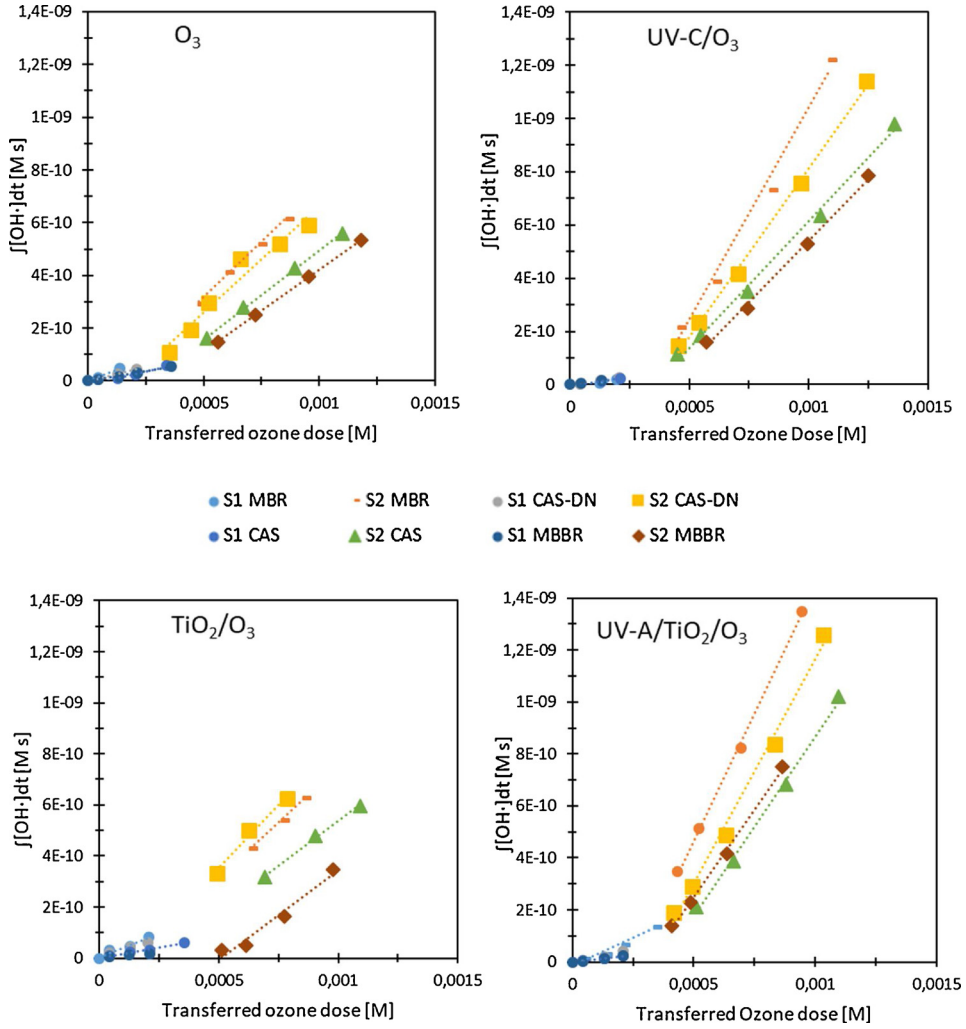

Fig. 2. R_{OHO3} plots for all experiments. Gas flow rate = 0.3 L min^{-1}; Inlet (g) ozone concentration = 10 mg O_3 L^{-1}; $T_{reaction}$ = 20 ± 2 °C; T_{in} (gas) = 22 ± 2 °C; P_{in} (gas) = 25 ± 2 mbar.

[45], less photons reached ACMP, producing lower degradation by that route. During stage 2, the turbidity of the medium and the ozone's reactivity with the matrices has been reduced. Consequently, more ozone is available for photolysis, thus increasing peroxide formation and consequently ˙OH generation (Eqs. (5) and (6)). Stage 2 R_{OHO3} values for UV-C/O_3 experiments were much higher than in single ozonation for all wastewaters (80% for MBR, 51% for CAS-DN; 37% for CAS and 43% for MBBR) indicating the expected increase on hydroxyl radical exposure per ozone consumed and the overall efficiency improvement of photolytic ozonation.

When TiO_2 is added to ozonation, stage 2 R_{OHO3} values increased slightly for all cases, while stage 1 value decreased for more polluted matrices CAS and MBBR. The understanding of this is limited due to the lack of data regarding heterogeneous catalytic ozonation performed in highly polluted wastewaters and the multiple interactions that might be taking place between light, ozone, the catalyst and the matrix. However, possible hypothesis is that the presence of TiO_2 may change the reactivity of molecular ozone with the matrix, thus affecting the R_{OHO3} value. Further studied should be performed in this direction.

The effect of photocatalytic ozonation on R_{OHO3} values was also much more significant during second stage. Stage 2 R_{OHO3} values for photocatalytic ozonation were the highest of all assayed processes–which can be explained by the multiple radical formation routes provided by the synergistic effect of ozonation and heterogeneous photocatalysis combined [23]. Thus, stage 2 R_{OHO3} values reached values higher than double for all wastewaters, compared with single ozonation (105% increase in CAs-DN and CAS; 121% increase in MBR and 127% increase in most polluted wastewater MBBR). These values confirm the importance of phtotocatalytic process on promoting the radical pathway in ozonation. On the other hand, stage 1 values for less turbid waters MBR and CAS-DN were higher than on single ozonation, most probably due to the smaller effect of organic matter and higher light absorption by TiO_2.

Table 3 also shows the amount of TOD needed to reach 65% of ACMP degradation for each process and matrix. As expected, less polluted matrices and light-assisted ozonation processes attaining higher R_{OHO3} needed less transferred ozone in general to reach this degradation value.

The results confirm that R_{OHO3} is an important parameter to determine the availability of hydroxyl radical on each wastewater matrix, being useful to compare radical production for each process and wastewater tested. It can also be used to predict the amount of TOD required for degrading ozone-resistant micropollutants during ozonation (Eq. (11)) [35,36]. Last assays were performed to evaluate the application of 2 stage R_{OHO3} values of MBR effluent for the prediction of atrazine removal. This pesticide presents low reactivity towards ozone, with second-order rate constant of $6\,M^{-1}\,s^{-1}$ and high reactivity with hydroxyl radicals ($k_{\cdot OH}$ of $3.0{\cdot}10^{9}\,M^{-1}\,s^{-1}$) [33]. Plots of the predicted and experimental atrazine abatement in ozonation and photocatalytic ozonation are presented in Fig. S12. In both cases, a good agreement between model predictions and experimental measurements was observed. Further experiments should be performed with different micropollutants for its final validation.

4. Conclusions

In this work, UV light-assisted ozonation processes attained higher degradation results of recalcitrant and ozone-resistant pesticide acetamiprid than single ozonation on real domestic wastewaters.

More polluted matrices had higher ozone transfer yields due to their reactivity with the oxidant. The presence of UV-C increased ozone consumption mass for all cases due to ozone photolysis, while adding UV-A in the presence of TiO_2 increased ozone consumption only for the less polluted matrices because they allowed a more efficient photocatalytic activity.

The adaptation of the $R_{OH,O3}$ concept presented good fitting results for all experiments, adopting ACMP as a probe compound. The plots had to be divided in two stages, before and after the corresponding IOD, due to the initial presence of highly reactive compounds towards molecular ozone in all wastewaters.

The improvement brought by both UV light-based processes on ACMP degradation was directly related with the increase in stage two R_{OHO3} values in all matrices. On that stage, photolytic ozonation values were up to 54% higher compared with single ozonation while for photocatalytic ozonation values were higher than double for all wastewaters studied (between 105–127%). These results demonstrate the capacity of light assisted ozonation processes on the enhancement of radical pathway degradation of ozone recalcitrant micropollutants, as well as the usefulness of modified R_{OHO3} parameter on its quantification. To take advantage of the improvements in radical production brought by UV light addition, the adoption of higher O_3 doses than the values typically used for ozonation in WWTPs is required.

Acknowledgments

This Special Issue is dedicated to honor the retirement of Prof. César Pulgarin at the Swiss Federal Institute of Technology (EPFL, Switzerland), a key figure in the area of Catalytic Advanced Oxidation Processes. This work was financially supported by the Spanish Ministry of Economy and Competitiveness (project CTQ2014-52607-R), AGAUR - Generalitat de Catalunya (project 20145GR245). This work was funded by the European Commission within the Erasmus+KA1 Programme, Erasmus Mundus Joint Master Degree in Chemical Innovation and Regulation.

Appendix A. Supplementary data

Supplementary material related to this article can be found, in the online version, at doi:https://doi.org/10.1016/j.apcatb.2019.02.072.

References

[1] Y. Luo, W. Guo, H. Ngo, L. Nghiem, F. Hai, J. Zhang, S. Liang, W. Wang, A review on the occurrence of micropollutants in the aquatic environment and their fate and removal during wastewater treatment, Sci. Total Environ. 473–474 (2014) 619–641, https://doi.org/10.1016/j.scitotenv.2013.12.065.

[2] M. Kim, K. Zoh, Occurrence and their removal of micropollutants in water environments, Environ. Eng. Res. 21 (4) (2016) 319–332, https://doi.org/10.4491/eer.2016.115.

[3] S. Kurwadkar, X. Zhang, D. Ramirez, F. Mitchell, Emerging micro-pollutants in the environment: occurrence, fate, and distribution, ACS Symposium Series, American Chemical Society, Washington, DC, 2015.

[4] B. Kasprzyk-Hordern, R. Dinsdale, A. Guwy, The occurrence of pharmaceuticals, personal care products, endocrine disruptors and illicit drugs in surface water in South Wales, Water Res. 42 (13) (2008) 3498–3518, https://doi.org/10.1016/j.watres.2008.04.026.

[5] K. Fent, A.A. Weston, D. Carminada, Ecotoxicology of human pharmaceuticals, Aquat. Toxicol. 76 (2006) 122–159, https://doi.org/10.1016/j.aquatox.2005.09.009.

[6] A. Mecha, M. Onyango, M. Momba, Impact of ozonation in removing organic micropollutants in primary and secondary municipal wastewater: effect of processes parameters, Water Sci. Technol. 74 (3) (2016) 756–765, https://doi.org/10.2166/wst.2016.276.

[7] J. Reungoat, B. Escher, M. Macova, F. Argaud, W. Gernjak, J. Keller, Ozonation and biological activated carbon filtration of wastewater treatment plant effluents, Water Res. 46 (3) (2012) 863–872, https://doi.org/10.1016/j.watres.2011.11.064.

[8] D. Gerrity, S. Gamage, J.C. Holady, D.B. Mawhinney, O. Quiñones, R.A. Trenholm, S. Snyder, Pilot-scale evaluation of ozone and biological activated carbon 632 for trace organic contaminant mitigation and disinfection, Water Res. 45 (2011) 2155–2165, https://doi.org/10.1016/10.1016/j.watres.2010.12.031.

[9] U. von Gunten, Ozonation of drinking water: part I. Oxidation kinetics and product formation, Water Res. 37 (2003) 1443–1467, https://doi.org/10.1016/S0043-1354(02)00457-8.

[10] M. Bourgin, B. Beck, M. Boehler, E. Borowska, J. Fleiner, E. Salhi, R. Teichler, U. von Gunten, H. Siegrist, C.S. McArdell, Evaluation of a full-scale wastewater treatment plant upgraded with ozonation and biological post-treatments: abatement of micropollutants, formation of transformation products and oxidation by-products, Water Res. 129 (2018) 486–498, https://doi.org/10.1016/J.WATRES.2017.10.036.

[11] P. Stathatou, F. Gad, E. Kampgragou, H. Grigoropoulou, D. Assimacopoulos, Treated wastewater reuse potential: mitigating water scarcity problems in the

Aegean Islands, Desal. Water Treat. J. 53 (12) (2015) 3272–3282, https://doi.org/10.1080/19443994.2014.934108.
[12] F. Beltran, Ozone Kinetics for Water and Wastewater Systems, CRC Press Lewis Publishers, 2004, pp. 193–227.
[13] M. Dodd, M. Buffle, U. von Gunten, Oxidation of antibacterial molecules by aqueous ozone: moiety-specific reaction kinetics and application to ozone-based wastewater treatment, Environ. Sci. Technol. 40 (2006) 1969–1977, https://doi.org/10.1021/es051369x.
[14] G.V. Buxton, C.L. Greenstock, W.P. Helman, A.B. Ross, Critical review of rate constants for reactions of hydrated electrons, hydrogen atoms and hydroxyl radicals in aqueous solution, J. Phys. Chem. Ref. Data 17 (1988) 513–886, https://doi.org/10.1063/1.555805.
[15] NDRL/NIST Solution Kinetics Database, http://kinetics.nist.gov/solution/. (Accessed 22 April 2018).
[16] J. Yang, U. Wu, H. Tai, W. Sheng, Effectiveness of an ultraviolet-C disinfection system for reduction of health-care associated pathogens, J. Microbiol. Immunol. Infect. (in press). https://doi.org/10.1016/j.jmii.2017.08.017.
[17] S. Satyro, E. Saggioro, F. Verissimo, D. Buss, D. Paiva Magalhaes, A. Oliveira, Triclocarban: UV photolysis, wastewater disinfection and ecotoxicology assessment using molecular biomarkers, Environ. Sci. Pollut. Res. Int. 24 (19) (2017) 16077–16085, https://doi.org/10.1007/s11356-017-9165-4.
[18] Z. Chen, J. Fang, C. Fan, S. Shang, Oxidative degradation of N-Nitrosopyrrolidine by the ozone/UV process: kinetics and pathways, Chemosphere 150 (2016) 731–739, https://doi.org/10.1016/j.chemosphere.2015.12.046.
[19] D. Robert, R. Daghirt, P. Drogui, Modified TiO_2 for environmental photocatalytic applications: a review, Ind. Eng. Chem. Res. 52 (10) (2013) 3581–3599, https://doi.org/10.1021/ie303468t.
[20] I. Ola, M. Maroto-Valer, Review of material design and reactor engineering on TiO_2 photocatalysis for CO_2 reduction, J. Photochem. Photobiol. C: Photochem. Rev. 24 (2015) 16–42, https://doi.org/10.1016/j.jphotochemrev.2015.06.00.
[21] J. Carbajo, A. Bahamonde, M. Faraldos, Photocatalyst performance in wastewater treatment applications: towards the role of TiO_2 properties, Mol. Catal. 434 (2017) 167–174, https://doi.org/10.1016/j.mcat.2017.03.018.
[22] A. Lisenbigler, G. Lu, J. Yates, Photocatalysis on TiO_2 surfaces: principles, mechanisms, and selected results, Chem. Rev. 95 (1995) 735–758, https://doi.org/10.1021/cr00035a013.
[23] Y. Guo, L. Yang, X. Cheng, X. Wang, The Application and reaction mechanism of catalytic ozonation in water treatment, J. Environ. Anal. Toxicol. 2 (2012) 150, https://doi.org/10.4172/2161-0525.1000150.
[24] E. Emam, Effect of ozonation combined with heterogeneous catalysts and ultraviolet radiation on recycling of gas-station wastewater, Egypt. J. Pet. 21 (1) (2012) 55–60, https://doi.org/10.1016/j.ejpe.2012.02.008.
[25] K.P. Yu, G. Whei-May Lee, G.H. Huang, The effect of ozone on the removal effectiveness of photocatalysis on indoor gaseous biogenic volatile organic compounds, J. Air Waste Manag. Assoc. 7 (201) (2010) 820–829, https://doi.org/10.3155/1047-3289.60.7.820.
[26] F. Parrino, G. Camera-Roda, V. Loddo, G. Palmisano, V. Augugliaro, Combination of ozonation and photocatalysis for purification of aqueous effluents containing formic acid as probe pollutant and bromide ion, Water Res. 50 (2014) 189–199, https://doi.org/10.1016/j.watres.2013.12.001.
[27] F. Beltran, A. Aguinaco, J. Garcia-Araya, Kinetic modelling of TOC removal in the photocatalytic ozonation of diclofenac aqueous solutions, Appl. Catal. B: Environ. 100 (1–2) (2010) 289–298, https://doi.org/10.1016/j.apcatb.2010.08.005.
[28] O. Eren, E. Kusvuran, A. Yildirim, S.A. Gul, Comparative study of ozonation, homogeneous catalytic ozonation, and photocatalytic ozonation for C.I. Reactive Red 194 azo dye degradation, Clean Soil Air Water 39 (8) (2011) 795–805, https://doi.org/10.1002/clen.201000192.
[29] R. Rajeswari, S. Kanmani, Degradation of pesticide by photocatalytic ozonation process and study of synergistic effect by comparison with photocatalysis and UV/ozonation processes, J. Adv. Oxid. Technol. 12 (2) (2009) 208–214, https://doi.org/10.1515/jaots-2009-0209.
[30] R. Solis, F. Rivas, J. Perez-Bote, O. Gimeno, Photocatalytic ozonation of 4-chloro-2-methylphenoxyacetic acid and its reaction intermediate 4-chloro-2-methyl phenol, J. Taiwan Inst. Chem. Eng. 46 (2015) 125–131, https://doi.org/10.1016/j.jtice.2014.09.010.
[31] O. Gimeno, F. Rivas, F. Beltran, M. Carbajo, Photocatalytic ozonation of winery wastewaters, J. Agric. Food Chem. 55 (24) (2007) 9944–9950, https://doi.org/10.1021/jf072167i.
[32] N. Moreira, J. Sousa, G. Macedo, A. Ribeiro, L. Barrieros, M. Pedrosa, J. Faria, M. Pereira, S. Castro-Silva, M. Segundo, C. Manaia, O. Nunes, A. Silva, Photocatalytic ozonation of urban wastewater and surface water using immobilized TiO_2 with LEDs: micropollutants, antibiotic resistance genes and estrogenic activity, Water Res. 94 (2016) 10–22, https://doi.org/10.1016/j.watres.2016.02.003.
[33] J. Acero, K. Stemmler, U. von Gunten, Degradation kinetics of atrazine and its degradation products with ozone and OH radicals: a predictive tool for drinking water treatment, Environ. Sci. Techol. 34 (2000) 591–597, https://doi.org/10.1021/es990724e.
[34] M.S. Elovitz, U. von Gunten, Hydroxyl radical/ozone ratios during ozonation processes. I. The Rct concept, Ozone Sci. Eng. 21 (3) (1999) 239–260, https://doi.org/10.1080/0191951990854723.
[35] M. Kwon, H. Kye, Y. Jung, Y. Yoon, H. Kang, Performance characterization and kinetic modeling of ozonation using a new method: R_{OHO3} concept, Water Res. 122 (2017) 172–182, https://doi.org/10.1016/j.watres.2017.05.062.
[36] A. Cruz-Alcalde, S. Esplugas, C. Sans, Abatement of ozone-recalcitrant micropollutants during municipal wastewater ozonation: kinetic modelling and surrogate-based control strategies, Chem. Eng. J. 170 (2019) 1092–1100, https://doi.org/10.1016/j.cej.2018.10.206.
[37] S. Canonica, L. Meunier, U. von Gunten, Phototransformation of selected pharmaceuticals during UV treatment of drinking water, Water Res. 42 (2008) 121–128, https://doi.org/10.1016/j.watres.2007.07.026.
[38] M. Marce, B. Domenjoud, S. Esplugas, S. Baig, Ozonation treatment of urban primary and biotreated wastewaters: impacts and modeling, Chem. Eng. J. 283 (2016) 768–777, https://doi.org/10.1016/j.cej.2015.07.073.
[39] A. Cruz-Alcalde, C. Sans, S. Esplugas, Priority pesticide abatement by advanced water technologies: the case of acetamiprid removal by ozonation, Sci. Total Environ. 599–600 (2017) 1454–1461, https://doi.org/10.1016/j.scitotenv.2017.05.065.
[40] D. Gardoni, R. Canziani, Decay of ozone in water: a review, Ozone Sci. Eng. 34 (4) (2012) 233–242, https://doi.org/10.1080/01919512.2012.686354.
[41] A. Yavas, Catalytic ozonation of paracetamol using commercial and Pt-supported nanocomposites of Al_2O_3: the impact of ultrasound, Ultrason. Sonochem. 40 (2018) 175–182, https://doi.org/10.1016/j.ultsonch.2017.02.017.
[42] R. Zhang, D. Yuan, B. Liu, Kinetics and products of ozonation of C.I. Reactive Red 195 in semi-batch reactor, Chin. Chem. Lett. 26 (1) (2015) 93–99, https://doi.org/10.1016/j.cclet.2014.10.024.
[43] W. Audenaert, Y. Vermeersch, Y. Van Hulle, P. Dejans, A. Dumoulin, I. Nopens, Application of a mechanistic UV/hydrogen peroxide model at full scale: sensitivity analysis, calibration and performance evaluation, Chem. Eng. J. 171 (1) (2011) 113–126, https://doi.org/10.1016/j.cej.2011.03.071.
[44] P. Andersen, C. Williford, J. Birks, Miniature personal ozone monitor based on UV absorbance, Anal. Chem. 82 (19) (2010) 7924–7928, https://doi.org/10.1021/ac1013578.
[45] S. Gora, S. Andrews, Adsorption of natural organic matter and disinfection byproduct precursors from surface water onto TiO_2 nanoparticles: pH effects, isotherm modelling and implications for using TiO_2 for drinking water treatment, Chemosphere 174 (2017) 363–370, https://doi.org/10.1016/j.chemosphere.2017.01.125.